# THERMAL DIFFUSION, HALL CURRENT AND CHEMICAL REACTION EFFECTS ON UNSTEADY MHD NATURAL CONVECTIVE FLOW PAST A VERTICAL PLATE

Malapati VENKATESWARLU[1], Dasari VENKATA LAKSHMI[2]

*The heat and mass transfer characteristics of the unsteady hydromagnetic natural convection flow with Hall current and Soret effect of an incompressible, viscous, electrically conducting, heat absorbing and radiating fluid flow past a suddenly started infinite vertical plate through fluid saturated porous medium in a rotating environment are taken into account in this paper. The exact analytical solutions of momentum, energy and concentration equations are obtained. The velocity, concentration and temperature profiles, Skin friction, Sherwood number and Nusselt number are easily examined and discussed via the closed forms obtained.*

**Keywords:** MHD fluid, Hall current, porous medium, thermal radiation, chemical reaction.

## Nomenclature

| | | | |
|---|---|---|---|
| $a^*$ | mean absorption coefficient | $K_1^*$ | dimensional permeability Parameter |
| $B_0$ | uniform magnetic field | $K_1$ | permeability of porous medium |
| $C^*$ | species concentration | $K_r^*$ | dimensional chemical reaction |
| $C_\infty^*$ | uniform concentration | $K_r$ | non-dimensional chemical reaction |
| $C_w^*$ | concentration of the wall | $k_T$ | thermal conductivity of the fluid |
| $c_p$ | specific heat at constant pressure | $M$ | magnetic parameter |
| $D_M$ | chemical molecular diffusivity | $m$ | hall current parameter |
| $G_m$ | Solutal Grashof number | $R$ | radiation parameter |
| $G_r$ | thermal Grashof number | $Nu$ | Nusselt number |
| $g$ | acceleration due to gravity | $P_r$ | Prandtl number |
| $j_w$ | mass flux | $Q_o$ | dimensional heat absorption |
| $K^2$ | rotation parameter | | |
| $q_w$ | heat flux | $q_r^*$ | radiating flux vector |
| $S_c$ | Schmidt number | $t$ | non - dimensional time |
| $Sh$ | Sherwood number | | |

[1] Assistant Professor, Department of Mathematics, V. R. Siddhartha Engineering College, Vijayawada, A.P, India, PIN: 520 007. Email: mvsr2010@gmail.com
[2] Professor, Department of Mathematics, Bapatla Women's Engineering College, Bapatla, Andhra Pradesh, India, PIN: 522 102. Email: himaja96@gmail.com

| | |
|---|---|
| $S_o$ | Soret number |
| $T_M$ | mean temperature of the fluid |
| $T^*$ | fluid temperature |
| $T_w^*$ | temperature of the wall |
| $T_\infty^*$ | uniform temperature |
| $t^*$ | dimensional time |

**Greek Symbols**

| | |
|---|---|
| $\alpha$ | dimensional thermal radiation parameter |
| $\beta_c$ | coefficient expansion for species concentration |
| $\beta_T$ | coefficient of thermal expansion |
| $\nu$ | kinematic coefficient of viscosity |
| $\omega$ | A scaled frequency |
| $\omega_e$ | cyclotron frequency |
| $\Omega$ | angular velocity |
| $t_o$ | characteristic time |
| $U_o$ | characterstic velocity |
| $u$ | primary velocity |
| $u^*$ | fluid velocity in $x^*$ – direction |
| $v^*$ | fluid velocity in $y^*$ – direction |
| $w^*$ | fluid velocity in $z^*$ – direction |
| $w$ | secondary velocity |
| $\phi$ | non – dimensional heat absorption |
| $\rho$ | fluid density |
| $\sigma$ | electrical conductivity |
| $\sigma^*$ | Stefan Boltzmann constant |
| $\tau$ | skin friction coefficient |
| $\tau_x$ | primary skin friction coefficient |
| $\tau_z$ | secondary skin friction coefficient |
| $\tau_e$ | electron collision time |
| $\tau_w$ | shear stres |

## 1. Introduction

It is observed that when the density of an electrically conducting fluid is low and/or applied magnetic field is strong, Hall current is produced in the flow-field which plays an important role in determining flow features of the problems because it induces secondary flow in the flow-field. Keeping in view this fact, significant investigations on hydromagnetic free convection flow past a flat plate with Hall effects under different thermal conditions are carried out by several researchers in the past. Mention may be made of the research studies of Pop and Watanabe [1], Abo-Eldahab and Elbarbary [2], Takhar et al. [3] and Saha et al. [4]. It is worthy to note that Hall current induces secondary flow in the flow-field which is also the characteristics of Coriolis force. Therefore, it becomes very important to compare and contrast the effects of these two agencies and also to study their combined effects on such fluid flow problems. Satya Narayana et al. [5] studied the effects of Hall current and radiation–absorption on MHD natural convection heat and mass transfer flow of a micropolar fluid in a rotating frame of reference. Seth et al. [6] investigated effects of Hall current and rotation on unsteady hydromagnetic natural convection flow of a viscous, incompressible, electrically conducting and heat absorbing fluid past an impulsively moving vertical plate with ramped temperature in a porous medium taking into account the effects of thermal diffusion.

Combined heat and mass transfer in fluid-saturated porous media finds applications in a variety of engineering processes such as heat exchanger devices,

petroleum reservoirs, chemical catalytic reactors and processes, geothermal and geophysical engineering, moisture migration in a fibrous insulation and nuclear waste disposal and others. Venkateswarlu et al. [7-14] presented heat and mass transfer effects on radiative MHD free convective non linear boundary layer flow past a permeable plate. Md Abdus Samad and Mohammad Mansur Rahman [15] studied the thermal radiation interaction with unsteady MHD flow past a vertical porous plate immersed in a porous medium**.** Makinde and Sibanda [16-17] studied on MHD boundary layer flow heat and mass transfer past a vertical plate in a porous medium with constant heat flux. By means of the presented solutions, the skin friction, heat transfer and mass transfer coefficients of physical importance can be rigorously investigated. The rest of the paper is organized as follows; section two presents the formation of the problem. Section three describes the method of solution and results are discussed in section four.

## 2. Mathematical formulation

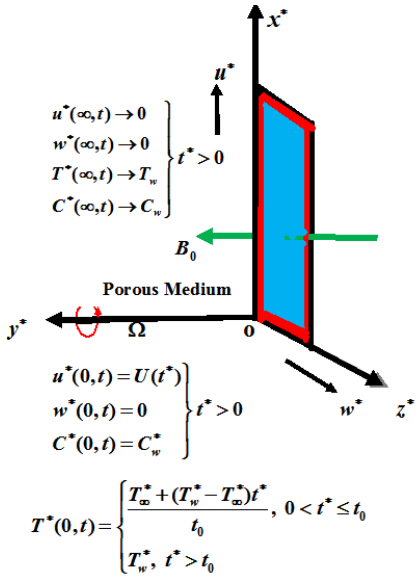


Fig.1: Physical model and coordinate system

We consider the unsteady radiative MHD natural convective flow of a viscous, incompressible and electrically conducting fluid past an infinite moving vertical porous plate. Under the assumptions made by Seth et al. [6], as well as of the usual Boussinesq's approximation, the governing equations can be expressed as:

Continuity equation:

$$\frac{\partial v^*}{\partial y^*} = 0 \tag{1}$$

Momentum conservation equations:

$$\frac{\partial u^*}{\partial t^*} + 2\Omega w^* = \nu \frac{\partial^2 u^*}{\partial y^{*2}} - \frac{\sigma B_0^2}{\rho}\left[\frac{u^* + m w^*}{1+m^2}\right] + g\beta_T\left(T^* - T_\infty^*\right) + g\beta_C\left(C^* - C_\infty^*\right) - \nu \frac{u^*}{K_1^*} \tag{2}$$

$$\frac{\partial w^*}{\partial t^*} - 2\Omega u^* = \nu \frac{\partial^2 w^*}{\partial y^{*2}} + \frac{\sigma B_0^2}{\rho}\left[\frac{m u^* - w^*}{1+m^2}\right] - \nu \frac{w^*}{K_1^*} \tag{3}$$

Energy conservation equation:

$$\frac{\partial T^*}{\partial t^*} = \frac{k_T}{\rho c_p}\frac{\partial^2 T^*}{\partial y^{*2}} - \frac{Q_0}{\rho c_p}\left(T^* - T_\infty^*\right) - \frac{1}{\rho C_p}\frac{\partial q_r^*}{\partial y^*} \tag{4}$$

Mass diffusion equation:

$$\frac{\partial C^*}{\partial t^*} = D_M \frac{\partial^2 C^*}{\partial y^{*2}} + \frac{D_M k_T}{T_M}\frac{\partial^2 T^*}{\partial y^{*2}} - K_r^*\left(C^* - C_\infty^*\right) \tag{5}$$

where $m = \omega_e \tau_e$ is Hall current parameter.

We should in prior warn the reader that our model is not the same as that by Seth et al. [6] in which the Soret and chemical reaction effects were not taken into account. Assuming that no slipping occurs between the plate and fluid, the corresponding initial and boundary conditions of the system of partial differential equations for the fluid flow problem are given below

$$\left.\begin{aligned}
&u^* = w^* = 0,\ T^* = T_\infty^*,\ C^* = C_\infty^* \text{ at } y^* \geq 0 \text{ and } t^* \leq 0\\
&u^* = U(t^*), w^* = 0, C^* = C_w^* \text{ at } y^* = 0 \text{ and } t^* > 0\\
&T^* = \frac{T_\infty^* + \left(T_w^* - T_\infty^*\right)t^*}{t_0} \text{ at } y^* = 0 \text{ and } 0 < t^* \leq t_0\\
&T^* = T_w^* \text{ at } y^* = 0 \text{ and } t^* > t_0\\
&u^* \to 0, w^* \to 0, T^* \to T_\infty^*, C^* \to C_\infty^* \text{ as } y^* \to \infty \text{ and } t^* > 0
\end{aligned}\right\} \tag{6}$$

Following Rapits [18], by using the Rosseland approximation, radiative flux vector $q_r$ can be written as:

$$\frac{\partial q_r^*}{\partial y^*} = -4a^*\sigma^*\left(T_\infty^{*4} - T^{*4}\right) \tag{7}$$

We assume that the difference between the fluid temperature and the free stream temperature is sufficiently small, such that expanding in Taylor's series $T^{*4}$ about $T_\infty^*$ and neglecting the second and higher order terms, $T^{*4}$ is expressed as

$$T^{*4} \approx 4T_\infty^{*3}T^* - 3T_\infty^{*4} \tag{8}$$

Using the equations (7) and (8) in the last term of equation (4) we obtain

$$\frac{\partial T^*}{\partial t^*} = \frac{k}{\rho c_p}\frac{\partial^2 T^*}{\partial y^{*2}} - \frac{Q_0}{\rho c_p}\left(T^* - T_\infty^*\right) - \frac{16a^*\sigma^* T_\infty^{*3}}{\rho C_p}\left(T^* - T_\infty^*\right) \tag{9}$$

In order to write the governing equations and the boundary conditions in non-dimensional form, the following non-dimensional quantities are introduced.

$$y = \frac{y^*}{U_0 t_0}, u = \frac{u^*}{U_0}, w = \frac{w^*}{U_0}, t = \frac{t^*}{t_0}, T = \frac{T^* - T_\infty^*}{T_w^* - T_\infty^*}, C = \frac{C^* - C_\infty^*}{C_w^* - C_\infty^*} \tag{10}$$

Equations (2), (3), (5) and (9) reduce to the following dimensional form.

$$\frac{\partial u}{\partial t} + 2K^2 w = \frac{\partial^2 u}{\partial y^2} - \frac{M(u + mw)}{1 + m^2} - \frac{u}{K_1} + G_r T + G_m C \tag{11}$$

$$\frac{\partial w}{\partial t} - 2K^2 u = \frac{\partial^2 w}{\partial y^2} + \frac{M(mu - w)}{1 + m^2} - \frac{w}{K_1} \tag{12}$$

$$\frac{\partial T}{\partial t} = \frac{1}{\mathrm{P}_r}\frac{\partial^2 T}{\partial y^2} - (R + \phi)T \tag{13}$$

$$\frac{\partial C}{\partial t} = \frac{1}{S_c}\frac{\partial^2 C}{\partial y^2} + S_0\frac{\partial^2 T}{\partial y^2} - K_r C \tag{14}$$

Here $K^2 = \frac{\Omega\nu}{U_0^2}, M = \frac{\sigma B_0^2 \nu}{\rho U_0^2}, K_1 = \frac{K_1^* U_0^2}{\nu^2}, G_r = \frac{g\beta_T \nu (T_w^* - T_\infty^*)}{U_0^3}, G_m = \frac{g\beta_C \nu (C_w^* - C_\infty^*)}{U_0^3},$

$\mathrm{Pr} = \frac{\nu\rho c_p}{k_T}, R = \frac{16a^*\sigma^*\nu T_\infty^*}{\rho c_p U_0^2}, \phi = \frac{\nu Q_0}{\rho c_p U_0^2}, Sc = \frac{\nu}{D_M}, S_0 = \frac{D_M k_T (T_w^* - T_\infty^*)}{T_M \nu (C_w^* - C_\infty^*)}, K_r = \frac{K_r^* \nu}{U_0^2}$

are the rotation parameter, magnetic parameter, permeability parameter, thermal Grashof number, Solutal Grashof number, Prandtl number, radiation parameter, heat absorption parameter, Schmidt number, Soret number and chemical reaction parameter respectively.

It is noticed that characteristic time $t_0$ may be defined according to the non-dimensional method mentioned above as

$$t_0 = \frac{\nu}{U_0^2} \tag{15}$$

The initial and boundary conditions, presented by equation (6) become

$$\left.\begin{array}{l} u=0,\ w=0,\ T=0,\ C=0 \ \text{ at } \ y\geq 0 \ \text{ and } \ t\leq 0 \\ u=f(t),\ \ w=0,\ \ C=1 \ \text{ at } \ y=0 \ \text{ and } \ t>0 \\ T=t \ \text{ at } \ y=0 \ \text{ and } \ 0<t\leq 1 \\ T=1 \ \text{ at } \ y=0 \ \text{ and } \ t>1 \\ u\to 0,\ \ w\to 0,\ \ T\to 0,\ \ C\to 0 \ \text{ as } \ y\to\infty \text{ and } t>0 \end{array}\right\} \tag{16}$$

where $f(t)=\dfrac{U(t^*)}{U_0}$

By combining the equations (11) and (12), we obtain

$$\frac{\partial F}{\partial t}-2iK^2F=\frac{\partial^2 F}{\partial y^2}-\left[N+\frac{1}{K_1}\right]F+G_rT+G_mC \tag{17}$$

where $F=u+iw$ and $N=\dfrac{M}{1+im}$.

The initial and boundary conditions, presented by equation (16), can be written as

$$\left.\begin{array}{l} F=0,\ \ T=0,\ \ C=0 \ \text{ at } \ y\geq 0 \ \text{ and } \ t\leq 0 \\ F=f(t),\ \ C=1 \ \text{ at } \ y=0 \ \text{ and } \ t>0 \\ T=t \ \text{ at } \ y=0 \ \text{ and } \ 0<t\leq 1 \\ T=1 \ \text{ at } \ y=0 \ \text{ and } \ t>1 \\ F\to 0,\ \ T\to 0,\ \ C\to 0 \ \text{ as } \ y\to\infty \text{ and } t>0 \end{array}\right\} \tag{18}$$

In order to investigate the flow features of the fluid generated due to uniformly accelerated movement of the plate, we consider $f(t)=R_1t$, where $R_1$ - a non-dimensional constant.

Given the velocity, temperature and concentration fields in the boundary layer, the shear stress $\tau_w$, the heat flux $q_w$ and mass flux $j_w$ are obtained by

$$\tau_w=\mu\left[\frac{\partial F}{\partial y}\right]_{y^*=0},\qquad q_w=-\alpha\left[\frac{\partial T}{\partial y}\right]_{y^*=0},\qquad j_w=-D_m\left[\frac{\partial C}{\partial y}\right]_{y^*=0} \tag{19}$$

In non-dimensional form the skin-friction coefficient $Cf$, heat transfer coefficient $Nu$ and mass transfer coefficient $Sh$ are defined as

$$Cf=\frac{\tau_w}{\rho v^2},\quad Nu=\frac{\nu}{U_o}\frac{q_w}{k_T\left(T_w^*-T_\infty^*\right)},\qquad Sh=\frac{\nu}{U_o}\frac{j_w}{D_m\left(C_w^*-C_\infty^*\right)} \tag{20}$$

Using non-dimensional variables in equation (10) and equation (19) into equation (20), we obtain the physical parameters

$$Cf=\left[\frac{\partial F}{\partial y}\right]_{y=0},\qquad Nu=-\left[\frac{\partial T}{\partial y}\right]_{y=0},\qquad Sh=-\left[\frac{\partial C}{\partial y}\right]_{y=0} \tag{21}$$

## 3. Solution of the problem

We assume the trial solutions for the velocity, temperature and concentration of the fluid as

$$F(y,t) = F_0(y)\exp(i\omega t) + o(\varepsilon^2) \tag{22}$$

$$T(y,t) = T_0(y)\exp(i\omega t) + o(\varepsilon^2) \tag{23}$$

$$C(y,t) = C_0(y)\exp(i\omega t) + o(\varepsilon^2) \tag{24}$$

where $\omega$ is frequency of oscillation and $\varepsilon << 1$ .

Substituting equations (22) to (24) into equations (13), (14) and (17), then equating the harmonic and non–harmonic terms and neglecting the higher order terms of $o(\varepsilon^2)$, we obtain

$$F_0'' - \left[ N + \frac{1}{K_1} + i\omega - 2iK^2 \right] F_0 = -(G_r T_0 + G_m C_0) \tag{25}$$

$$T_0'' - P_r(R + \phi + i\omega)T_0 = 0 \tag{26}$$

$$C_0'' - S_c(K_r + i\omega)C_0 = -S_c S_0 T_0'' \tag{27}$$

where prime denotes the ordinary differentiation with respect to $y$ .

The corresponding initial and boundary conditions can be written as

$$\left.\begin{array}{lll} F_0 = 0, \quad T_0 = 0, \quad C_0 = 0 & \text{at} & y \geq 0 \text{ and } t \leq 0 \\ F_0 = f(t)\exp(-i\omega t), \quad C_0 = \exp(-i\omega t) & \text{at} & y = 0 \text{ and } t > 0 \\ T_0 = t\exp(-i\omega t) & \text{at} & y = 0 \text{ and } 0 < t \leq 1 \\ T_0 = \exp(-i\omega t), & \text{at} & y = 0 \text{ and } t > 1 \\ F_0 \to 0, \quad T_0 \to 0, \quad C_0 \to 0 & \text{as} & y \to \infty \text{ and } t > 0 \end{array}\right\} \tag{28}$$

Solving equations (25) – (27) under the boundary conditions (28), we obtain the solutions for velocity, temperature and concentration distribution in the boundary layer as

$$F(y,t) = A_{12}\exp(-A_6 y) + A_{10}\exp(-A_1 y) + A_8\exp(-A_2 y) \tag{29}$$

$$T(y,t) = t\exp(-A_1 y) \tag{30}$$

$$C(y,t) = A_5\exp(-A_2 y) + A_4\exp(-A_1 y) \tag{31}$$

Here $A_1 = \sqrt{P_r(R + \phi + i\omega)}$, $A_2 = \sqrt{S_c(K_r + i\omega)}$, $A_3 = S_c S_0$, $A_4 = \dfrac{A_1^2 A_3 t}{A_2^2 - A_1^2}$,

$A_5 = 1 - A_4$, $A_6 = \sqrt{N + \dfrac{1}{K_1} + i\omega - 2iK^2}$, $A_7 = \dfrac{G_r t}{A_6^2 - A_1^2}$, $A_8 = \dfrac{G_m A_5}{A_6^2 - A_2^2}$,

$$A_9 = \frac{G_m A_4}{A_6^2 - A_1^2}, A_{10} = A_7 + A_9, A_{11} = A_8 + A_{10}, A_{12} = R_1 t - A_{11}$$

Keeping in view the assumptions made earlier, solutions to the fluid velocity, temperature and concentration profiles in the case of isothermal plate are obtained and presented in the following form

$$F(y,t) = A_{21}\exp(-A_6 y) + A_{19}\exp(-A_{13} y) + A_{17}\exp(-A_2 y) \tag{32}$$

$$T(y,t) = \exp(-A_{13} y) \tag{33}$$

$$C(y,t) = A_{15}\exp(-A_2 y) + A_{14}\exp(-A_{13} y) \tag{34}$$

Here $A_{13} = \sqrt{P_r(R+\phi)}, A_{14} = \frac{A_3 A_{13}^2}{A_2^2 - A_{13}^2}, A_{15} = 1 - A_{14}, A_{16} = \frac{G_r}{A_6^2 - A_{13}^2},$

$$A_{17} = \frac{G_m A_{15}}{A_6^2 - A_2^2}, A_{18} = \frac{A_{14} G_m}{A_6^2 - A_{13}^2}, A_{19} = A_{16} + A_{18}, A_{20} = A_{17} + A_{19}, A_{21} = R_1 t - A_{20}$$

### 3.1 Skin Friction, Nusselt Number and Sherwood number

Skin friction for ramped temperature plate:

$$\tau = \tau_x + i\tau_z = \left[\frac{\partial F}{\partial y}\right]_{y=0} = -\left[A_6 A_{12} + A_1 A_{10} + A_2 A_8\right] \tag{35}$$

Skin friction for isothermal plate:

$$\tau = \tau_x + i\tau_z = \left[\frac{\partial F}{\partial y}\right]_{y=0} = -\left[A_6 A_{21} + A_{13} A_{19} + A_2 A_{17}\right] \tag{36}$$

Nusselt number for ramped temperature plate:

$$N_u = -\left[\frac{\partial T}{\partial y}\right]_{y=0} = tA_1 \tag{37}$$

Nusselt number for isothermal plate:

$$N_u = -\left[\frac{\partial T}{\partial y}\right]_{y=0} = A_{13} \tag{38}$$

Sherwood number for ramped temperature plate:

$$S_h = -\left[\frac{\partial C}{\partial y}\right]_{y=0} = A_2 A_5 + A_1 A_4 \tag{39}$$

Sherwood number for isothermal plate:

$$S_h = -\left[\frac{\partial C}{\partial y}\right]_{y=0} = A_2 A_{15} + A_{13} A_{14} \tag{40}$$

## 4. Graphical Results and Discussion

In order to investigate the influence of various physical parameters on the flow field, fluid primary velocity $u$, secondary velocity $w$, temperature $T$ and concentration $C$ have been studied analytically and computed results of the analytical solutions are displayed graphically from Figs.2 to 38. In the present study following default parameter values are adopted for computations: $M = 15.0$, $G_r = 4.0, G_m = 3.0, \mathrm{P}_r = 0.71, R = 2.0, R_1 = 1.0, \omega = 0.1, K_r = 0.5, K^2 = 2.0, S_c = 0.60,$ $t = 0.5, K_1 = 0.2, \phi = 3.0, m = 0.5$ and $S_0 = 1.0$. Therefore all the graphs and tables correspond to these values unless specifically indicated on the appropriate graph or table.

It is evident from Figs. 2 and 3 that, primary velocity $u$ increases on increasing Hall current parameter $m$ in a region near to the plate and it decreases on increasing $m$ in the region away from the plate whereas secondary velocity $w$ increases on increasing Hall current parameter $m$ throughout the boundary layer region for both ramped temperature and isothermal plates.

It is perceived from Figs .4 and 5 that, fluid primary velocity $u$ decreases on increasing rotation parameter $K^2$ whereas fluid secondary velocity $w$ increases on increasing $K^2$ for both ramped temperature and isothermal plates. This implies that, rotation tends to retard fluid primary velocity whereas it has a reverse effect on fluid secondary velocity for both ramped temperature and isothermal plates throughout the boundary layer region. This is due to the reason that Coriolis force is dominant in the region near to the axis of rotation.

The nature of fluid primary velocity $u$, secondary velocity $w$ and concentration $C$ in presence of foreign species such as Hydrogen $(S_c = 0.22)$, Helium $(S_c = 0.30)$, Water vapour $(S_c = 0.60)$, Ammonia $(S_c = 0.78)$ is shown in Figs 6 to 8 for both ramped temperature and isothermal plates. Physically, Schmidt number $S_c$ signifies the relative strength of viscosity to chemical molecular diffusivity. It is observed that, $u$, $w$ and $C$ increases on increasing $S_c$ in a region near to the plate and decreases on increasing $S_c$ in the region away from the plate for both ramped temperature and isothermal plates.

Figs. 9 and 10 depict the effect of Soret number $S_0$ on the fluid primary velocity $u$ and secondary velocity $w$ of the flow field for both ramped temperature and isothermal plates. It is seen, that primary velocity $u$ and secondary velocity $w$ increases on increasing the Soret number $S_0$ throughout the boundary layer region.

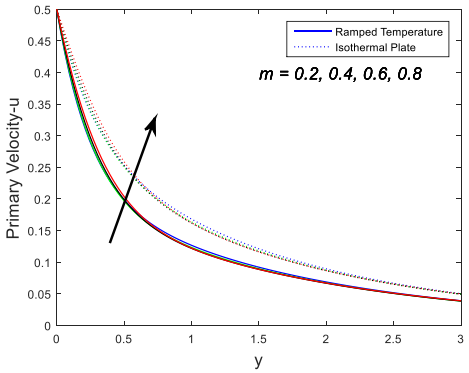


Fig. 2: Influence of $m$ on $u$.

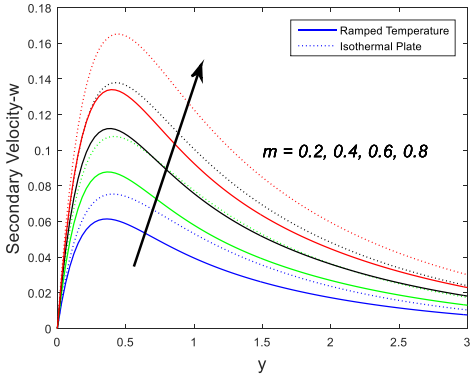


Fig 3: Influence of $m$ on $w$.

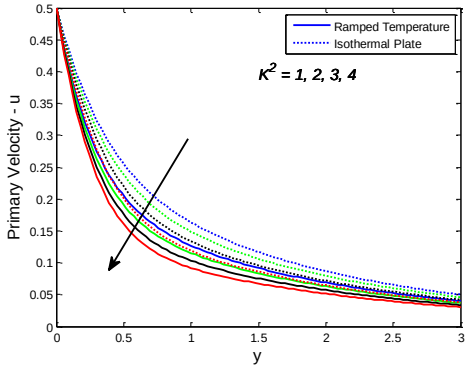


Fig 4: Influence of $K^2$ on $u$.

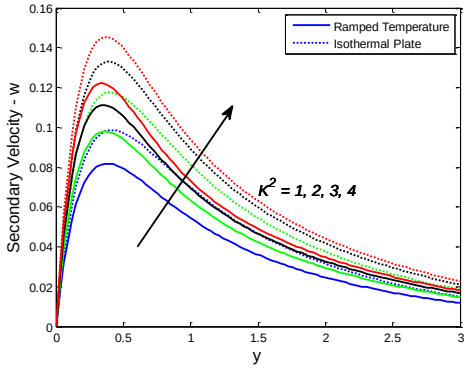


Fig 5: Influence of $K^2$ on $w$.

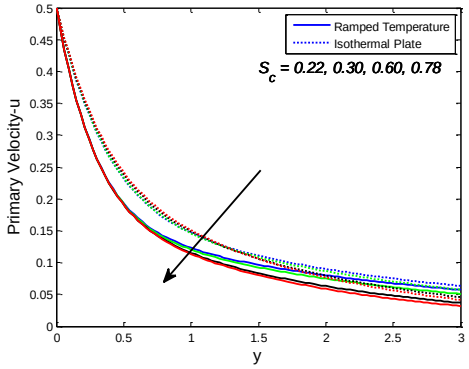


Fig.6: Influence of $S_c$ on $u$.

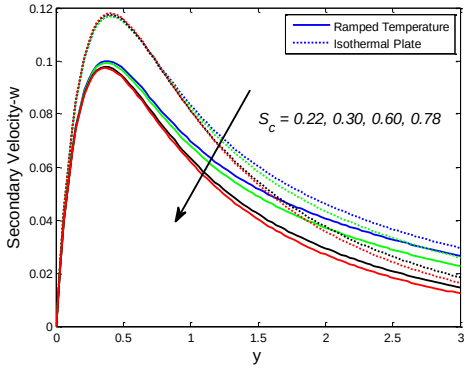


Fig.7: Influence of $S_c$ on $w$.

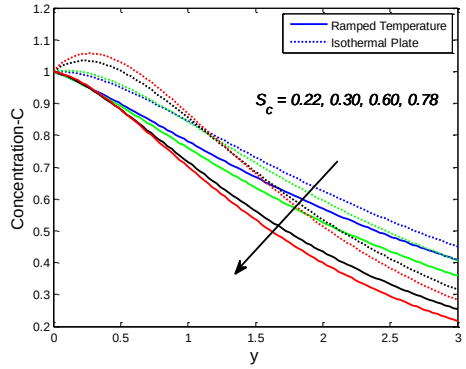


Fig.8: Influence of $S_c$ on $C$ .

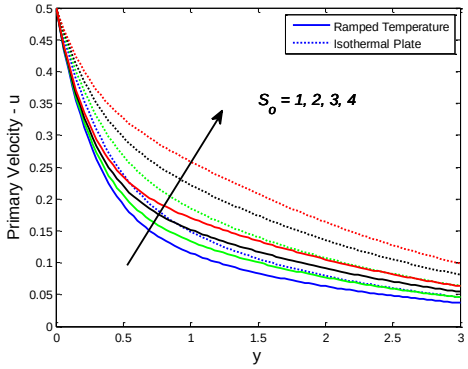


Fig.9: Influence of $S_o$ on $u$ .

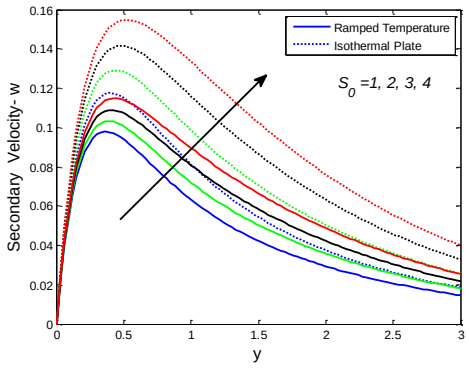


Fig.10: Influence of $S_o$ $w$ .

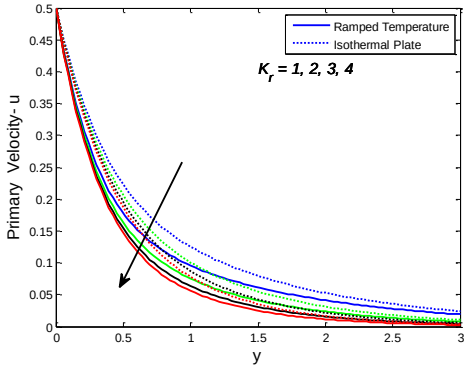


Fig.11: Influence of $K_r$ on $u$ .

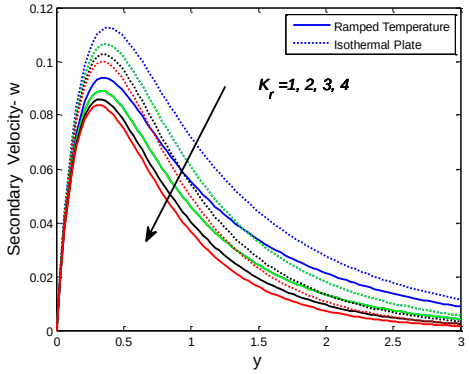


Fig.12: Influence of $K_r$ on $w$ .

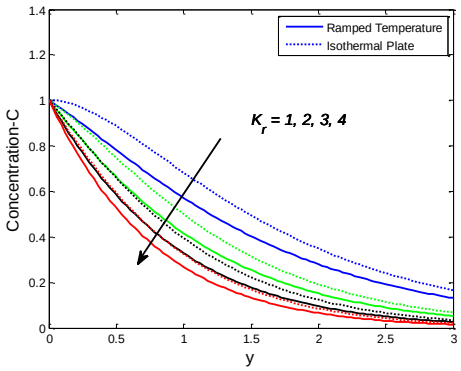


Fig.13: Influence of $K_r$ on $C$ .

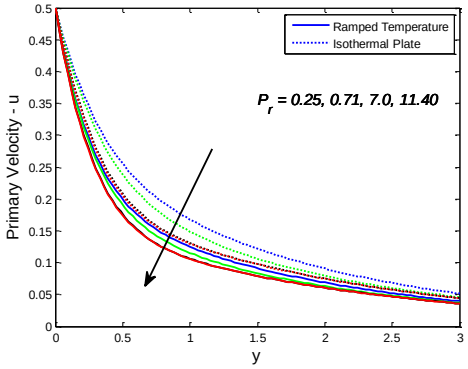


Fig.14: Influence of $P_r$ on $u$ .

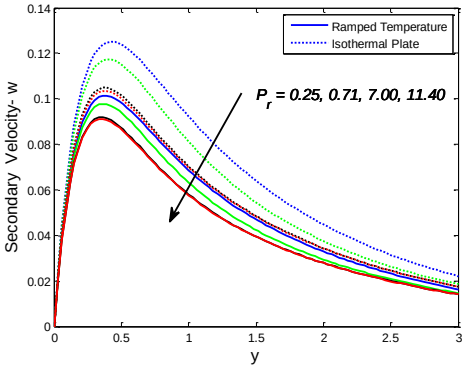


Fig.15: Influence of $P_r$ on $w$ .

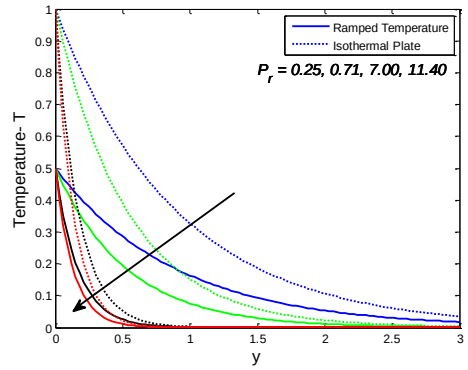


Fig.16: Influence of $P_r$ on $T$ .

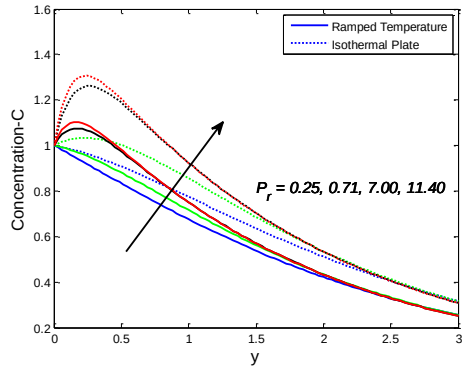


Fig.17: Influence of $P_r$ on $C$ .

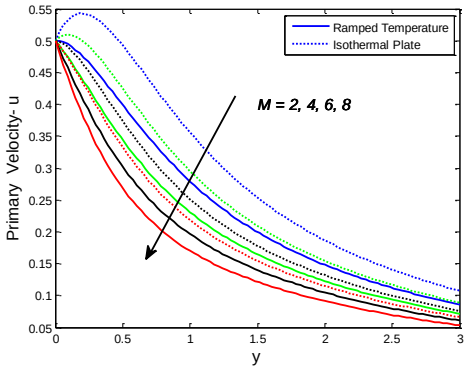


Fig.18: Influence of $M$ on $u$ .

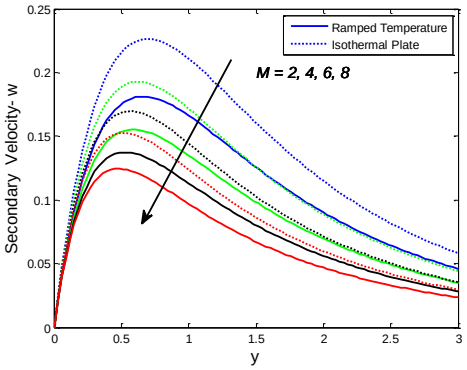


Fig.19: Influence of $M$ on $w$

Figs. 11 to 13 demonstrate the influence of chemical reaction parameter $K_r$ on fluid primary velocity $u$ , secondary velocity $w$ and concentration $C$ of the flow field for both ramped temperature and isothermal plates. It is seen, that fluid primary

velocity $u$, secondary velocity $w$ and concentration $C$ decreases with increasing the chemical reaction parameter $K_r$ for both ramped temperature and isothermal plates.

*Table 1*

**Skin friction coefficient at ramped temperature plate and isothermal plate when $G_r = 4.0$, $K^2 = 2.0, R = 2.0, \phi = 3.0, m = 0.5, S_c = 0.60$, $t = 0.5$, $G_m = 3.0$, $R_1 = 1.0$, $\omega = 0.1$.**

| $S_o$ | $K_r$ | $P_r$ | $K_1$ | $M$ | Ramped temperature | | Isothermal plate | |
|---|---|---|---|---|---|---|---|---|
| | | | | | $\tau_x$ | $\tau_z$ | $\tau_x$ | $\tau_z$ |
| 1.0 | 0.5 | 0.71 | 0.2 | 15.0 | -1.1983 | 0.7866 | -0.8461 | 0.8618 |
| 2.0 | 0.5 | 0.71 | 0.2 | 15.0 | -1.1593 | 0.8029 | -0.7679 | 0.8937 |
| 3.0 | 0.5 | 0.71 | 0.2 | 15.0 | -1.1204 | 0.8192 | -0.6898 | 0.9255 |
| 4.0 | 0.5 | 0.71 | 0.2 | 15.0 | -1.0815 | 0.8355 | -0.6117 | 0.9574 |
| 1.0 | 1.0 | 0.71 | 0.2 | 15.0 | -1.2277 | 0.7751 | -0.8804 | 0.8484 |
| 1.0 | 2.0 | 0.71 | 0.2 | 15.0 | -1.2643 | 0.7599 | -0.9224 | 0.8308 |
| 1.0 | 3.0 | 0.71 | 0.2 | 15.0 | -1.2893 | 0.7496 | -0.9506 | 0.8191 |
| 1.0 | 4.0 | 0.71 | 0.2 | 15.0 | -1.3086 | 0.7418 | -0.9722 | 0.8102 |
| 1.0 | 0.5 | 0.25 | 0.2 | 15.0 | -1.1739 | 0.7975 | -0.7973 | 0.8834 |
| 1.0 | 0.5 | 0.71 | 0.2 | 15.0 | -1.1983 | 0.7866 | -0.8461 | 0.8618 |
| 1.0 | 0.5 | 7.00 | 0.2 | 15.0 | -1.2665 | 0.7647 | -0.9824 | 0.8182 |
| 1.0 | 0.5 | 11.40 | 0.2 | 15.0 | -1.2812 | 0.7615 | -1.0116 | 0.8118 |
| 1.0 | 0.5 | 0.71 | 2.0 | 15.0 | -0.8655 | 0.9434 | -0.4859 | 1.0455 |
| 1.0 | 0.5 | 0.71 | 4.0 | 15.0 | -0.8462 | 0.9542 | -0.4650 | 1.0581 |
| 1.0 | 0.5 | 0.71 | 6.0 | 15.0 | -0.8398 | 0.9578 | -0.4581 | 1.0624 |
| 1.0 | 0.5 | 0.71 | 8.0 | 15.0 | -0.8366 | 0.9597 | -0.4546 | 1.0646 |
| 1.0 | 0.5 | 0.71 | 0.2 | 2.0 | 0.0077 | 0.7605 | 0.5041 | 0.8738 |
| 1.0 | 0.5 | 0.71 | 0.2 | 4.0 | -0.2443 | 0.7513 | 0.2169 | 0.8541 |
| 1.0 | 0.5 | 0.71 | 0.2 | 6.0 | -0.4614 | 0.7506 | -0.0283 | 0.8457 |
| 1.0 | 0.5 | 0.71 | 0.2 | 8.0 | -0.6532 | 0.7548 | -0.2433 | 0.8438 |

Figs. 14 to 17 demonstrate the plot of primary velocity $u$, secondary velocity $w$, Temperature $T$ and concentration $C$ for both ramped temperature and isothermal plates of the flow field against different values of Prandtl number $P_r$ taking other parameters are constant. The Prandtl number defines the ratio of momentum diffusivity to thermal diffusivity. The values of the Prandtl number are chosen for air ($P_r = 0.71$), electrolytic solution ($P_r = 1.00$), water ($P_r = 7.00$) and water at $4^0C$ ($P_r = 11.40$). It is observed that, the primary velocity $u$, secondary velocity $w$, and temperature $T$ of the flow field decreases in magnitude as Prandtl number $P_r$ increases where as concentration $C$ increases on increasing the Prandtl

number $P_r$ for both ramped temperature and isothermal plates throughout the boundary layer region.

*Table 2*

**The local heat transfer coefficient $N_u$ for various values of $R, P_r$ and $\phi$.**

| $R$ | $P_r$ | $\phi$ | Nusselt number $N_u$ | |
|---|---|---|---|---|
| | | | Ramped temperature | Isothermal plate |
| 10.0 | 0.71 | 3.0 | 1.5191 | 3.0381 |
| 20.0 | 0.71 | 3.0 | 2.0205 | 4.0410 |
| 30.0 | 0.71 | 3.0 | 2.4202 | 4.8405 |
| 40.0 | 0.71 | 3.0 | 2.7627 | 5.5254 |
| 2.0 | 0.25 | 3.0 | 0.5591 | 1.1180 |
| 2.0 | 0.71 | 3.0 | 0.9422 | 1.8841 |
| 2.0 | 7.00 | 3.0 | 2.9583 | 5.9161 |
| 2.0 | 11.40 | 3.0 | 3.7753 | 7.5498 |
| 2.0 | 0.71 | 1.0 | 0.7299 | 1.4595 |
| 2.0 | 0.71 | 3.0 | 0.9422 | 1.8841 |
| 2.0 | 0.71 | 4.0 | 1.0321 | 2.0640 |
| 2.0 | 0.71 | 9.0 | 1.3973 | 2.7946 |

*Table 3*

**The local mass transfer coefficient $S_h$ for various values of $S_c, K_r$ and $S_o$.**

| $S_c$ | $K_r$ | $S_0$ | Sherwood number $S_h$ | |
|---|---|---|---|---|
| | | | Ramped temperature | Isothermal plate |
| 0.22 | 0.5 | 1.0 | 0.1608 | 0.0426 |
| 0.30 | 0.5 | 1.0 | 0.1600 | 0.0918 |
| 0.60 | 0.5 | 1.0 | 0.1276 | 0.3324 |
| 0.78 | 0.5 | 1.0 | 0.1030 | 0.4825 |
| 0.60 | 1.0 | 1.0 | 0.3772 | 0.0562 |
| 0.60 | 2.0 | 1.0 | 0.7388 | 0.3826 |
| 0.60 | 3.0 | 1.0 | 1.0119 | 0.6821 |
| 0.60 | 4.0 | 1.0 | 1.2392 | 0.9292 |
| 0.60 | 0.5 | 1.0 | 0.1276 | 0.3324 |
| 0.60 | 0.5 | 2.0 | 0.3303 | 1.2021 |
| 0.60 | 0.5 | 3.0 | 0.7645 | 2.0760 |
| 0.60 | 0.5 | 4.0 | 1.2009 | 2.9504 |

It is noticed from Figs.18 and 19 that, the primary velocity $u$ and secondary velocity $w$ decrease on increasing the magnetic parameter $M$ for both ramped temperature and isothermal plates. This implies that magnetic field tends to

decelerate fluid flow in both the primary and secondary flow directions throughout the boundary layer region. This is due to the fact that application of a magnetic field to an electrically conducting fluid gives rise to a mechanical force, called Lorentz force, which has a tendency to resist fluid motion in the flow field.

The numerical values of primary skin friction $\tau_x$ and secondary skin friction $\tau_z$ for both ramped temperature and isothermal plates are presented in table 1. It is clear that the primary skin friction $\tau_x$ increases on increasing $S_o$ and $K_1$ whereas it decreases on increasing $K_r, P_r$ and $M$ for both ramped temperature and isothermal plates. From the results, in table 2, mass transfer coefficient $N_u$ increases on increasing $R, P_r$ and $\phi$ for both ramped temperature and isothermal plates. It is clear from table 3, Sherwood number $S_h$ increases on increasing $K_r$ and $S_o$ for both ramped temperature and isothermal plates. Sherwood number $S_h$ decreases on in increasing Schmidt number $S_c$ for ramped temperature plate whereas it has a reverse effect on isothermal plate.

## REFERENCES


[1] *I Pop and T. Watanabe:* Hall effect on magnetohydrodynamic free convection about a semi-infinite vertical flat plate, Int. J. Eng Sci, vol. 32, 1994, pp. 1903–1911.

[2] *Abo-Eldahab and E. M. E Elbarbary:* Hall current effect on magnetohydrodynamic free-convection flow past a semi infinite vertical plate with mass transfer, Int. J. Eng Sci, vol. 39, 2001, pp. 1641–1652.

[3] *H. S. Takhar, S. Roy and G. Nath:* Unsteady free convection flow over an infinite vertical porous plate due to the combined effects of thermal and mass diffusion, magnetic field and Hall currents, Int. J. Heat and Mass Transfer, vol. 39, 2003, pp. 825–834.

[4] *L. K. Saha, S. Siddiqa and M. A. Hossain:* Effect of Hall current on MHD natural convection flow from vertical permeable flat plate with uniform surface heat flux, Appl. Math Mech Engg Ed, vol. 32, 2011, pp. 127–146.

[5] *P. V. Satya Narayana, B. Venkateswarlu and S. Venkataramana:* Effects of Hall current and radiation absorption on MHD micropolar fluid in a rotating system, Ain Shams Eng J, vol. 4, 2013, pp. 843–854.

[6] *G. S. Seth, G. K. Mahato and S. Sarkar:* Effects of Hall current and rotation on MHD natural convection flow past an impulsively moving vertical plate with ramped temperature in the presence of thermal diffusion with heat absorption, Int. J. Energy Tech, vol. 5, 2013, pp. 1–12.

[7] *M. Venkateswarlu, D. Venkata Lakshmi and G. Darmaiah*: Influence of slip condition on radiative MHD flow of a viscous fluid in a parallel porous plate channel in presence of heat absorption and chemical reaction , J. Korean Soc. Ind. Appl. Math., vol. 20, no. 4, 2016, pp. 333 -354.

[8] *M. Venkateswarlu and D. Venkata Lakshmi*: Dufour effect on radiative MHD flow of a viscous fluid in a parallel porous plate channel under the influence of slip condition, Journal of Advances in Science and Technology., vol. 12, no. 25, 2016, pp. 614 -620.

[9] *M. Venkateswarlu and P. Padma:* Unsteady MHD free convective heat and mass transfer in a boundary layer flow past a vertical permeable plate with thermal radiation and chemical reaction, Procedia Engineering, vol. 127, 2015, pp. 791-799.

[10] *J. Manjula, P. Padma, M. Gnaneswara Reddy and M. Venakateswarlu:* Influence of thermal radiation and chemical reaction on MHD flow, heat and mass transfer over a stretching surface, Procedia Engineering, vol.127, 2015, pp. 1315-1322.

[11] *M. Venkateswarlu, G. V. Ramana Reddy and D. V. Lakshmi:* Radiation effects on MHD boundary layer flow of liquid metal over a porous stretching surface in porous medium with heat generation, J. Korean Soc. Ind. Appl. Math., vol. 19, 2015, pp.83-102.

[12] *M. Venkateswarlu, G. V. Ramana Reddy and D. V. Lakshmi:* Thermal diffusion and radiation effects on unsteady MHD free convection heat and mass transfer flow past a linearly accelerated vertical porous plate with variable temperature and mass diffusion, J. Korean Soc. Ind. Appl. Math., vol.18, 2014, pp. 257-268.

[13] *M. Venkateswarlu, G. V. Ramana Reddy and D. V. Lakshmi:* Diffusion-thermo effects on MHD flow past an infinite vertical porous plate in the presence of radiation and chemical reaction, International Journal of Mathematical Archive, vol. 4, 2013, pp. 39-51.

[14] *M. Venkateswarlu, G. V. Ramana Reddy and D. V. Lakshmi:* Effects of chemical reaction and heat generation on MHD boundary layer flow of a moving vertical plate with suction and dissipation, Engineering International, vol. 1, 2013, pp.27-38.

[15] *Md Abdus Samad and Mohammad Mansur Rahman:* Thermal radiation interaction with unsteady mhd flow past a vertical porous plate immersed in a porous medium, Journal. Naval Architecture and Marine Engineering, vol. 3, no. 1, 2006, pp. 7-14.

[16] *O. D. Makinde:* On MHD boundary layer flow and mass transfer past a vertical plate in a porous medium with constant heat flux, International Journal of Numerical Method for Heat and Fluid Flow, vol. 19, 2009, pp. 546-554.

[17] *O. D. Makinde and P. Sibanda:* Magnetohydrodynamic mixed convective flow and heat transfer past a vertical plate in a porous medium with constant wall suction, ASME J. Heat Transfer, vol. 130, no. 11, 2008, pp. 112602 (1-8).

[18] *A. Raptis:* Free convective oscillatory flow and mass transfer past a porous plate in the presence of radiation for an optically thin fluid, Thermal Sci., vol. 15, 2011, pp. 849-857.